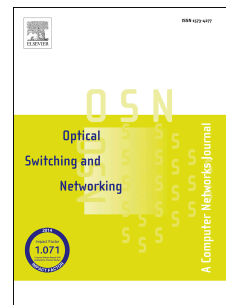


# Journal Pre-proof

Novel Evolutionary Planning Technique for Flexible-grid Transmission in Optical Networks

Matheus R. Sena, Pedro J. Freire, Leonardo D. Coelho, Alex F. Santos, Antonio Napoli, Raul C. Almeida, Jr.



PII: S1573-4277(21)00045-X

DOI: <https://doi.org/10.1016/j.osn.2021.100648>

Reference: OSN 100648

To appear in: *Optical Switching and Networking*

Received Date: 14 February 2021

Revised Date: 20 July 2021

Accepted Date: 16 September 2021

Please cite this article as: M.R. Sena, P.J. Freire, L.D. Coelho, A.F. Santos, A. Napoli, R.C. Almeida Jr., Novel Evolutionary Planning Technique for Flexible-grid Transmission in Optical Networks, *Optical Switching and Networking*, <https://doi.org/10.1016/j.osn.2021.100648>.

This is a PDF file of an article that has undergone enhancements after acceptance, such as the addition of a cover page and metadata, and formatting for readability, but it is not yet the definitive version of record. This version will undergo additional copyediting, typesetting and review before it is published in its final form, but we are providing this version to give early visibility of the article. Please note that, during the production process, errors may be discovered which could affect the content, and all legal disclaimers that apply to the journal pertain.

© 2021 Elsevier B.V. All rights reserved.

**Matheus Sena:** Conceptualization, Methodology, Writing- Original draft preparation, Software, Data curation.

**Pedro Freire:** Conceptualization, Methodology, Writing- Original draft preparation, Software.

**Leonardo Coelho:** Writing- Reviewing and Editing.

**Alex Santos:** Data curation.

**Antonio Napoli:** Writing- Reviewing and Editing.

**Raul Almeida:** Conceptualization, Methodology, Writing- Original draft preparation, Supervision.

Journal Pre-proof

# Novel Evolutionary Planning Technique for Flexible-grid Transmission in Optical Networks

Matheus R. Sena<sup>a,b</sup>, Pedro J. Freire<sup>c</sup>, Leonardo D. Coelho<sup>a</sup>, Alex F. Santos<sup>d</sup>, Antonio Napoli<sup>e</sup> and Raul C. Almeida Jr<sup>a</sup>

<sup>a</sup>Department of Electronics and Systems, Universidade Federal de Pernambuco, Av. da Arquitetura, s/n, 50740-550, Recife-PE, Brazil

<sup>b</sup>now with Fraunhofer Institute for Telecommunications Heinrich Hertz Institute, Einsteinufer 37, 10587 Berlin, Germany,

<sup>c</sup>Aston University, Aston St, B4 7ET, Birmingham, United Kingdom

<sup>d</sup>Science and Technology Center on Energy and Sustainability, Federal University of Recôncavo da Bahia, Feira de Santana - BA, Brazil

<sup>e</sup>Infinera, Sankt-Martinstr. 76, 81541, Munich, Germany

Corresponding author: [matheus.sena@hhi.fraunhofer.de](mailto:matheus.sena@hhi.fraunhofer.de)

## ARTICLE INFO

### Keywords:

Elastic Optical Networks; Network Planning; Physical layer impairment; GN-model; Genetic Algorithms.

## ABSTRACT

This paper proposes a novel joint resource allocation technique for flexible-grid systems by utilizing non-dominant sort genetic algorithm (NSGA-II) in a multi-objective optimization framework. It pioneers the implementation of an evolutionary mechanism to optimize resources as means of mitigation of physical layer impairments. This investigation initially introduces a proposal in which bandwidth reduction, maximization of the minimum signal-to-noise ratio (SNR) margin, and minimization/maximization of the sum of SNR margins are studied under dual-objective Pareto analysis in the link-level scenario. Later, the technique extends existing provisioning strategies for network planning by targeting the reduction of blocking and spectral utilization of optical connections.

## 1. Introduction

The dynamism of today's data traffic demands has motivated the development of more flexible and faster telecommunication systems to cope with the heterogeneity of services and escalating requirements of user's consumption habits. In these systems, the necessity of physical-layer-aware methods to improve quality of transmission (QoT) becomes critical in order to integrate the underlying transmission aspects into the network planning [1, 2] and provide more reliable resource allocation. In this regard, the emergence of channel models [3] that can accurately estimate physical layer impairments, especially nonlinear interference (NLI), has offered a framework where provisioning strategies can rapidly assess the QoT and provide more efficient decisions.

NLI in optical transmission is a theme that has been around in the field of optical communications since the early 90s [4]. Nevertheless, it was a while back when a reasonably accurate and low complexity model, named Gaussian noise (GN) [3], was proposed and later applied on several works [5, 6, 7] that combine it to diverse transmission scenarios. In a general sense, this model proposes treating the noise generated during the propagation of light as the sum of a contribution derived from the linear regime, originated in optical amplifiers (e.g., Erbium doped fiber amplifier (EDFA)), and a portion that arises from the nonlinear physical interaction between fiber and light. The latter is subdivided into two types of effects: self-channel interference (SCI), which comprises the noise that the optical channel triggers on itself, and cross-channel interference (XCI), that considers the mutual

interaction of neighboring channels. To deal with these impairments, the design of physical-layer-aware resource allocation techniques has become of key importance in the scope of Optical Networks.

A brief survey in the literature shows that the term "Resource Allocation" is predominantly observed in the process of assigning network assets (e.g., spectrum, route) to support strategic goals, i.e., maximize the signal-to-noise ratio (SNR) margin, minimize the total allocated bandwidth, etc. Numerous techniques have been extensively employed in optical communications to optimize resource allocation in network traffic, such as linear/nonlinear programming [6, 7] and metaheuristics. The latter is based on stochastic optimization inspired from miscellaneous fields (e.g., Game Theory [8], Swarm Intelligence [9, 10], Evolutionary Algorithms [11]) and has given evidence of aptness in providing a derivative-free method that yields sufficiently good results with incomplete datasets or limited computation capacity.

The method derived in this manuscript proposes the usage of an evolutionary metaheuristic – the non-dominated sorting genetic algorithm II (NSGA-II [12]) – to optimize resource allocation for offline planning when applied to point-to-point and meshed networks. This paper compares its numerical results with the benchmark provided by [6], given that analogous scenarios are assumed. Three Pareto analyses for the link-level approach are described. The first analysis focuses on the conflicting relationship between the minimization of total bandwidth vs. maximization of the minimum SNR margin. The second maintains the minimization of the total bandwidth, but it maximizes the sum of SNR margins. The third investigation is proposed to minimize the sum of SNR

ORCID(s):

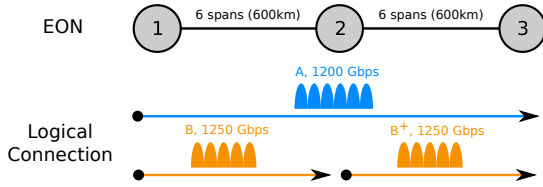


**Figure 1:** Optical link and channel configuration, where EON stands for Elastic Optical Network.

margins while maximizing the minimum SNR margin. The latter is a reformulation of what is proposed in [6], in which one of the main goals is to maximize the SNR margins of all channels, condition that may lead to over-provisioning of resources. As a result of this reformulation, spectrum resource savings can be obtained for specific transmission intervals. At last, the evolutionary algorithm provides a more substantial whole-network planning strategy, where the provisioning is adapted to optimize the blocking and total spectral usage for various meshed network topologies.

The remainder of the paper is structured as followed. Sec. 2 presents the optimization problem and the elements of nonlinear channel model theory needed for this work. In Sec. 3, the results for the link-level optimization are introduced, while Sec. 4 extends the algorithm to be applied in meshed networks. Finally, Sec. 5 draws the conclusions.

## 2. Optimization Process

### 2.1. Problem Statement

In the following analysis, we considered the same network topology of [6], which is portrayed by Fig. 1. In this point-to-point, there are three types of channels. Channels of type *A* (in blue) propagate from nodes 1 to 3. Channels of type *B* (in orange) are available for only half of the total network length, i.e., from node 1 to 2. At last, channels of type *B*<sup>+</sup> (the symmetric representation of *B*, also in orange) go from node 2 to 3. Channel *A* demands a bit rate of 200 Gbps, whereas *B* and *B*<sup>+</sup> of 250 Gbps. As degrees of freedom, it is possible to change the launch power and bandwidth (via adaptive modulation as described in Sec. 2.3.4) of each channel. Given that the purpose of this manipulation is to guarantee sufficient QoT to all carriers, it is necessary that the following inequality be obeyed:

$$\text{SNR}_i(\mathbf{c}, \mathbf{f}, \mathbf{G}) \geq \text{SNR}_{thr}(c_i) \quad (1)$$

Here,  $\text{SNR}_i(\mathbf{c}, \mathbf{f}, \mathbf{G})$  is the SNR calculated for the *i*-th channel as a function of the possible modulation formats ( $\mathbf{c} = (c_1, \dots, c_N)$ ,  $c$ : spectral efficiency (bits/s/Hz)), central frequencies ( $\mathbf{f} = (f_1, \dots, f_N)$ ), and power spectral density ( $\mathbf{G} = (G_1, \dots, G_N)$ ). Thereby, in a complementary way, some targets in the optimization description need to be included, and these are:

- minimize the total bandwidth occupied by channels,

$$\min_{\mathbf{c}} \sum_{i=1}^N R_i / 2c_i \quad (2)$$

where  $R_i$  is the data rate of the *i*-th channel and  $N$  is the total number of channels,

- maximize SNR margin of the most penalized channel,

$$\max_{\mathbf{c}, \mathbf{G}} \Delta \text{SNR}_{min} \quad (3)$$

where  $\Delta \text{SNR}_{min}$  corresponds to the minimum SNR margin,

- maximize the sum of the SNR margins of all channels.

$$\max_{\mathbf{c}, \mathbf{G}} \sum_{i=1}^N \Delta \text{SNR}_i \quad (4)$$

where  $\Delta \text{SNR}_i$  corresponds to the *i*-th channel SNR margin. In this work, we consider a null guardband between consecutive channels, such that  $\mathbf{f}$  is a function of  $\mathbf{c}$  and  $f_1 = 193.55$  THz. For that reason, we omit  $\mathbf{f}$  in the following formulations.

The multi-objective treatment of these variables ( $\mathbf{c}$  and  $\mathbf{G}$ ) is described in [6] and all formerly mentioned optimization targets are addressed. However, this is achieved via the aid of adjustment coefficients within a single cost function, which unveils a weighted single-objective optimization method. Given that the aim is to optimize a single cost function and promote no trade-off analysis, this assumption does not correspond to multi-objective premises. Furthermore, the choice of the optimization coefficients is empirical and it creates an environment where the solutions are optimal regarding the corresponding set of values. At last, another drawback found in [6] is the dependence on a MINLP tool [13], which increases the degree of implementation complexity. On the contrary, the technique derived within this work was implemented in a few lines of code and included as an additional feature to the SIMTON simulation tool [14].

### 2.2. Channel Model

As this work also focuses on the nonlinear impact of light propagation, the computation of the power spectral density originated from the nonlinearity of the *i*-th channel after  $N_s$  spans ( $G_{NLI,i}$ ) is mathematically given by the so-called incoherent Gaussian noise (IGN) model, summarized in equations 41–43 in [3], where equation 42 indirectly defines the XCI contribution, whilst 43 the SCI. With the computation of these nonlinear parcels, it is possible to estimate one of the fundamental variables discussed in this paper, the SNR margin ( $\Delta \text{SNR}$ ), which has a direct relation with the propagation reach. Margin dependence on the number of spans plays an important role to evaluate how far channels can propagate before crossing the SNR threshold ( $\text{SNR}_{thr}$ ) because of the additive incoherent accumulation of the nonlinear and ASE (amplified stimulated emission) noise. The SNR margin,

Physical parameters considered in this work	
Parameter	Value
$\alpha$	$0.22 \text{ dB} \times \text{km}^{-1}$
$\beta_2$	$-2.13 \text{ s}^{-2} \times \text{m}^{-1}$
$\gamma$	$1.3 \text{ W} \times \text{km}^{-1}$
	5 dB
	22 dB
$N_{s,1-2}, N_{s,2-3}$	6
$N_{s,1-3}$	12

**Table 1**

Summary of the physical parameters considered in this work.  $\alpha$ : fiber attenuation coefficient,  $\beta_2$ : fiber chromatic dispersion coefficient,  $\gamma$ : fiber nonlinear coefficient,  $N_{s,1-2}$ ,  $N_{s,2-3}$ ,  $N_{s,1-3}$ : number of spans from node 1 to 2, 2 to 3 and 1 to 3.

corresponding to the  $i$ -th channel after  $N_s$  spans, in linear units, is given by:

$$\Delta \text{SNR}_{i,N_s} = \frac{G_{ch,i}}{(G_{ASE,i,N_s} + G_{NLI,i}) \text{SNR}_{thr_i}}. \quad (5)$$

$G_{ASE,i,N_s}$  is approximately given by:  $N_s F_n (\Gamma_n - 1) f_{ch,i} h$ , where  $F_n$  is the  $n$ -th amplifier noise figure,  $\Gamma_n$  is the  $n$ -th amplifier gain,  $f_{ch,i}$  is the center frequency of the  $i$ -th channel and  $h$  is Planck's constant. Additionally, the considered SNR threshold values ( $\text{SNR}_{thr_i}$ ) are referenced in [15] (for a pre-FEC BER of  $4 \times 10^{-3}$ ) and differ according to the modulation format assumed by the channel. In this work we also considered that the amplifier gain is set such to compensate for the fiber attenuation loss. Table 1 summarizes the network physical parameters utilized in this work.

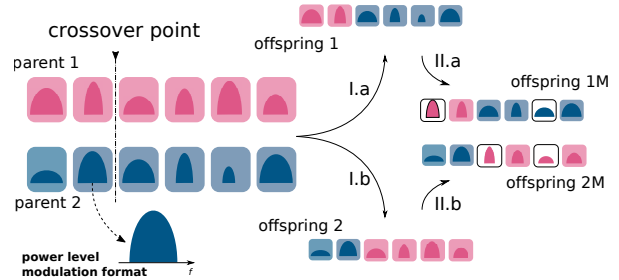
In network planning, the SNR is more often used as metric for QoT investigations, since with it, one can simply estimate the SNR Margin (Eq. 5). Maintaining the SNR margin above zero is an indication that after the FEC (forward error correction) decoding an error-free transmission can be obtained. Therefore, this supports the reason why we consider the SNR margin as an appropriate metric to be analyzed in the following studies.

### 2.3. Similarities with Genetic Features

A parallel between the optical spectrum and a chromosome will be drawn hereafter as means to justify the implementation of the NSGA-II. The corresponding illustration that correlates these two worlds is depicted in Fig. 2.

#### 2.3.1. Genes

Genes represent the basic and functional unit of heredity and are composed of a sequence of nucleobases that, according to the arrangement, determine different features of an individual. Similarly, optical channels are the fundamental physical units of transmission packages designated by different arrangements of design parameters. For instance, an optical channel can support different orders of modulation format (e.g., 4QAM, 8QAM, 16QAM), launch powers (e.g., 0 dBm, -5 dBm),

**Figure 2:** Parallel between genetic features and the optical framework.

frequencies, and the combination of each feature value identifies a specific carrier (gene).

#### 2.3.2. Chromosome

It is a linear sequence of concatenated genes. When translating to the optical context, it is the portion of the spectrum occupied by the transmitted optical channels. It will be referenced by the term "individual" in the next subsections.

#### 2.3.3. Crossover

This genetic operator can be described as the physical combination of sequences of genes from two different chromosomes to generate the offspring. In this particular process, the exchanged sequences of genes are determined by the crossover point (stochastically determined). Mirroring this mechanism to the optical context, the generated offspring can be understood via operations I.a and I.b in Fig. 2, where a set of channels from a sequence whose name is parent 1 (parent 2) is swapped with the complementary sequence of channels from parent 2 (parent 1). This operation generates the individuals named offspring 1 and offspring 2.

#### 2.3.4. Mutation

It is a random alteration of gene features. It can be illustrated by the operations II.a and II.b in Fig. 2. The square blocks, with a white background enclosing the optical channels, represent the mutated channels. In this work, a mutation probability  $Pr_M$  (per gene) determines the occurrence of this event. This means that each channel in offspring 1 and 2 has a  $Pr_M$  chance of having one of the features (i.e., modulation format, launch power) changed. The value of  $Pr_M$  is optimized and discussed in Sec. 3.1.

After this brief parallel between genes and optical channels, besides the operations (crossover and mutation) that rule the genetic evolution, it is clear that the algorithm should provide means of yielding new individuals more prone to environmental requirements (objective functions). It means the goal is that the iteration process results in multiple sets of optical channels (with numerous modulation formats and launch power values) that address the targets described in Sec. 2.1.

## 2.4. NSGA-II

The genetic algorithm applied in this study was the NSGA-II (non-dominated sorting genetic algorithm II) [12] and its foundations are based on the concept of non-dominance. NSGA-II also carries the core of multi-objective premises for the analysis here reported. In this approach, a notion widely used in Economics, Pareto's front [16], is applied. This concept is built upon the argument that a state of distribution of resources (objectives) is designed where it is impossible to relocate an individual to a better position (in terms of one of the resources) without worsening at least one of the others.

NSGA-II adds two other tasks after the Mutation and Crossover, which are: 1) Fast Non-dominated Sorting and 2) Crowding Distance. The former is responsible for determining the individuals on the Pareto's front. These individuals compose a set of solutions that are non-dominated, which means that no objective can be improved without sacrificing at least one of the other objectives. The latter task (Crowding Distance) is in charge of capping the number of possible solutions and avoids that the algorithm selects individuals in densely populated areas. This is an instrumental way to grant the diversity of solutions with multiplicity of features. In this task, every channel is associated with a metric called Hypervolume [17].

The Hypervolume is a metric inherent to every individual and is defined by the product of the absolute distances (in terms of objectives) between the previous and posterior individuals ( $i - 1$ ,  $i + 1$ ) regarding the  $i$ -th solution. Given that a  $P$ -dimensional space can be used, an expression for the  $i$ -th individual Hypervolume ( $V_i$ ) reads as follows:

$$V_i = \prod_{n=1}^P |f_{Obj_n}(i + 1) - f_{Obj_n}(i - 1)| \quad (6)$$

where  $f_{Obj_n}$  is the function that quantifies the  $n$ -th objective in the optimization problem.

## 2.5. Algorithms

To address the targets previously discussed in Sec. 2.1, namely, minimization of the total bandwidth occupied by channels ( $f_{Obj_1} = \sum_{i=1}^N R_i/2c_i$ ), maximization of the margin of SNR of the most penalized channel ( $f_{Obj_2} = \Delta SNR_{min}$ ) and, finally, maximization of the sum of the SNR margins ( $f_{Obj_3} = \sum_{i=1}^N \Delta SNR_i$ ), this paper proposes to treat the conflicting relations in a multi-objective optimization. Then, it is clear that the conflicting relations are between  $f_{Obj_1}$  vs.  $f_{Obj_2}$  and  $f_{Obj_1}$  vs.  $f_{Obj_3}$ . At last, another conflict is added in this paper, which is when the maximization of the margin of SNR of the most penalized channel ( $f_{Obj_2}$ ) is contrasted with the minimization of the sum of the SNR margins ( $f_{Obj_3}$ ).

In total, each individual is built on 16 types of channels, i.e., 6  $A$ , 5  $B$ , and 5  $B^+$ . Given that channels  $B$  and  $B^+$  are symmetrical, the analysis is made for 11 channels ( $N_{channels}$ )

and not for 16. All individual's channels are initialized with a random modulation format, i.e., PM-4QAM, PM-8QAM, PM-16QAM, or PM-32QAM), respectively represented in Algorithm 1 line 4 by  $c_1, c_2, c_3, c_4$ , and a constant power level ( $-20$  dBm, Algorithm 1 line 5).

---

### Algorithm 1 Initialization

---

```

1: Given  $N_{individuals}$  and  $N_{channels}$ 
2: while  $individual_i \leq N_{individuals}$  do
3:   while  $channel_j \leq N_{channels}$  do
4:      $modulation_j = U[c_1, c_2, c_3, c_4]$ 
5:      $power_j = -20$  dBm
6:   end while
7: end while

```

---

After the initialization, individuals start interacting in an evolutionary process as described in Algorithm 2. The total number of iterations ( $N_{iterations}$ ) was set to a maximum of 2000.

In Algorithm 2, the crossover mechanism is described from lines 3 to 7. In this process, it is necessary to group all individuals in pairs ( $pair_j = [parent_{j,1}, parent_{j,2}]$ , line 3) and permit the exchange of optical channels (lines 5). At the end of the process, the total number of individuals is  $2N_{individuals}$  (parents + offspring).

The mutation process is described from lines 9 to 21. The channels in all individuals ( $parents + offspring$ , in total  $2N_{individuals}$ ), at the end of the previous step, are exposed to a possibility of mutation ( $Pr_M$ , line<sup>1</sup> 10) and if that occurs (lines 11 to 20), an alteration probability ( $Pr_{a|M}$ , line 11) will define what type of change takes place. A probability of occurrence of 1/3 is given to all three types of alteration, i.e., power mutation (lines<sup>2</sup> 12 and 13.), only modulation format (lines<sup>3</sup> 14 and 15) and the joint modification of power and modulation (lines 16-18).

The Fast Non-dominated Sorting step is carried out in lines 23 and 24. At this moment, the algorithm has generated a total of individuals of  $4N_{individuals}$ , which corresponds to the original parents, offspring generated in the crossover process, mutated parents, and mutated offspring. The process of checking dominance consists of searching for solutions (designated by index  $i$ ) that permit no individual (designated by index  $j$ ) to perform the following:

$$f_{Obj_p}(individual_i) \geq f_{Obj_p}(individual_j) \cap f_{Obj_q}(individual_i) \leq f_{Obj_q}(individual_j) \quad (7)$$

To illustrate this operation with a more familiar scenario, suppose the case to be analyzed is  $f_{Obj_1}$  vs.  $f_{Obj_2}$ , in other words, minimization of the total bandwidth vs.

<sup>1</sup> $U(0, 1)$  represents a random variable uniformly distributed between 0 and 1.

<sup>2</sup>power increment/decrement  $\pm\sigma_p$  (the sign  $\pm$  is randomly set each time this operation occurs, line 13)

<sup>3</sup> $U[c_1, c_2, c_3, c_4]$  represents a random variable uniformly distributed over the four possible values of spectral efficiency  $c_1, c_2, c_3$  and  $c_4$ .

**Algorithm 2** Evolution

```

1: Given:  $N_{iterations}$ ,  $Pr_M$  and  $\sigma_p$ 
2: while  $iteration_i \leq N_{iterations}$  do
3:   group individuals in pairs
4:   while  $pair_j \leq N_{individuals}/2$  do
5:     exchange channels between  $pair_{j,1}$  and  $pair_{j,2}$ 
6:     generate  $of\ spring_{j,1}$  and  $of\ spring_{j,2}$ 
7:   end while
8:   while  $individual_j \leq 2N_{individuals}$  do
9:     while  $channel_k \leq N_{channels}$  do
10:      if  $U(0,1) \leq Pr_M$  then
11:         $Pr_{a|M} = U(0,1)$ 
12:        if  $Pr_{a|M} \leq 1/3$  then
13:           $power_k = power_k \pm \sigma_p$ 
14:        else if  $Pr_{a|M} > 1/3$  and  $Pr_{a|M} \leq 2/3$  then
15:           $modulation_k = U[c_1, c_2, c_3, c_4]$ 
16:        else
17:           $power_k = power_k + \sigma_p$ 
18:           $modulation_k = U[c_1, c_2, c_3, c_4]$ 
19:        end if
20:      end if
21:    end while
22:  end while
23:  while  $individual_j \leq 4N_{individual}$  do
24:    check dominance of the individualj
25:  end while
26:  while  $individuals_j \leq N_{stored}$  do
27:    calculate Hypervolumej
28:  end while
29:  choose  $N_{individuals}$  with highest Hypervolume values
30: end while

```

maximization of worst-case SNR margin. Any individual  $i$  that satisfies these conditions for both objectives over the entire population is considered non-dominated, i.e., there is no  $j$  such that satisfies the dominance criterion. After all non-dominated individuals are selected, they are collected in a set of  $N_{stored}$  candidate solutions.

In the last task (Crowding Distance), the algorithm calculates the Hypervolumes for all  $N_{stored}$  candidates (lines 26 and 27) and selects only  $N_{individuals}$  solutions with the highest Hypervolume values (line 29). The new  $N_{individuals}$  individuals are be used as input to the next iteration of the algorithm (line 2). A flowchart (Fig. 3) of the joint operation of Algorithm 1 and Algorithm 2 is added to facilitate the comprehension of the logic employed for the NSGA-II.

### 3. Numerical results

#### 3.1. Hyperparameter Optimization

The selection of some of the algorithm's most important parameters ( $\sigma_p$ ,  $N_{individuals}$ ,  $Pr_M$ ) is a Hyperparameter Tuning (HT) problem [18]. To solve it, we carried out a grid-search assuming:  $N_{individuals} \in \{25, 50, 100\}$ ,  $Pr_M \in \{2.5\%, 10\%, 40\%\}$  and

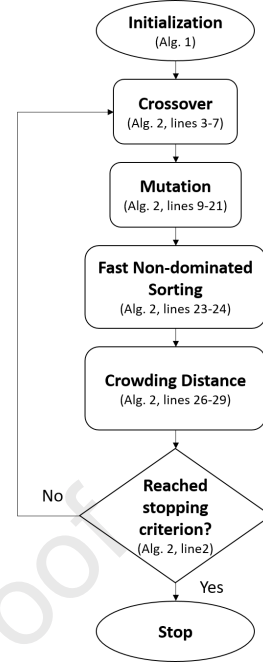


Figure 3: Flowchart of the NSGA-II. Alg.: Algorithm.

$\sigma_p \in \{-20, -10, 0, 10\}$  dBm to minimize the required number of iterations in a pre-computed channel configuration scenario where the solution is known *a priori*. After this optimization was executed, the set [ $N_{individuals} = 50$ ,  $Pr_M = 10\%$ ,  $\sigma_p = -10$  dBm] was found to achieve the expected solution with the least amount of iterations.

#### 3.2. Algorithm's Complexity

The complexity of the NSGA-II basically depends on three important variables: the number of iterations ( $N_{iterations}$ ), the number of individuals ( $N_{individuals}$ ) and the size of the individuals ( $n$ ). Therefore, the complexity is on the order of  $\mathcal{O}(N_{iterations}N_{individuals}n)$ . Another important factor is the complexity of the fitness function, which in this work corresponds to the calculation of the total bandwidth (in  $f_{obj_1}$ ) and the calculation of the SNR for all optical channels (in  $f_{obj_2}$  and  $f_{obj_3}$ ). However, the aforementioned fitness evaluations are negligible in comparison to the complexity imposed by the crossover and mutation processes. In the results presented over the next three subsections (3.3, 3.4, 3.5), we considered  $N_{iterations} = 2000$ ,  $N_{individuals} = 50$  and  $n = 22$  (corresponding to the power levels and modulation formats of all eleven channels A/A<sup>+</sup> and B/B<sup>+</sup>). The optimizations were run on a 16 GB RAM memory computer and the 2000 iterations lasted approximately 1.5 hours.

#### 3.3. Total bandwidth vs. Minimum SNR Margin

In this section, the algorithm was applied to obtain solutions that analyze the Pareto's relation between minimizing the total bandwidth and maximizing the lowest SNR margin. This approach meets the necessary conflict

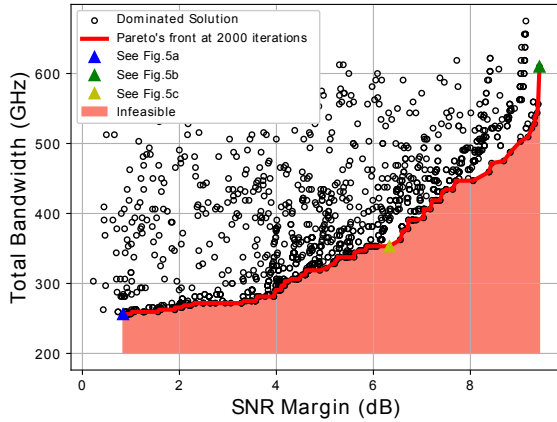


**Figure 4:** Pareto's front for the multi-objective optimization. Minimum SNR margin vs. Total Bandwidth.

requirements in a Pareto analysis because the reduction of bandwidth forces the algorithm to use more efficient modulation formats, which consequently lowers the overall SNR margin performance. For the results presented in this and in the following sections, we assumed that the physical parameters were the same as used in [6] and summarized in Table 1.

As it can be explained by observing Fig. 4, the Pareto's front determines the border of feasible solutions. All black markers represent a sample of individuals that have been at some point dominated by more recent generations. It is also possible to analyze two opposing solutions that lie on the extreme sides of the curve, i.e., the one that prioritizes the bandwidth (leftmost and depicted by Fig. 5.a) and the one that prioritizes SNR margin (rightmost and depicted by Fig. 5.b).

As expected, to reduce the bandwidth, the algorithm delivers an individual with higher spectral efficiency (SE) modulation formats (Fig. 5.a), in this case PM-32QAM<sup>1</sup>. To prioritize the maximization of the lowest SNR margin, the spectrum is composed uniquely by PM-4QAM channels (Fig. 5.b) given that the SNR threshold is lower, thus permitting resourceful solutions in terms of margin. At last, a hybrid solution (Fig. 5.c) has been shown to exemplify how the algorithm distributes different modulation formats over the channels to address a specific bandwidth + margin requirement when neither the bandwidth nor the lowest SNR margin is prioritized. Besides, it also accounts for the fact that the channel *A* propagates over a longer distance and therefore more robust modulation formats (PM-8QAM) are required when compared to channels *B/B+* (PM-16QAM). The values of the objectives for the three individuals (Fig. 5.a-c) are summarized in Table 2.

<sup>1</sup>Note that PM-32QAM was the considered modulation format with the highest SE in the results shown in subsections 3.3-5.

Relation between individual and objective function		
Individual represented by	SNR Margin (dB)	Total BW (GHz)
Fig. 5.a	1	250
Fig. 5.b	9.5	612.5
Fig. 5.c	6.2	350

**Table 2**

Quantitative comparison between the individuals (Fig. 5.a-c) and their respective values of objective functions. BW: bandwidth.

Relation between individual and objective function		
Individual represented by	Sum of SNR Margin (linear)	Total BW (GHz)
Fig. 6.a	25	250
Fig. 6.b	185	612.5

**Table 3**

Quantitative comparison between the individuals (Fig. 6.a, b) and their respective values of objective functions. BW: bandwidth.

### 3.4. Total bandwidth vs. Sum of SNR Margins

The second conflicting relation analyzed in this paper considers the minimization of the total bandwidth and the maximization of the sum of SNR margins. Regarding the previous approach, this maximization reveals a concern with the overall performance of channels and not only with the most penalized. Nevertheless, this can lead to a sub-optimal distribution of margins throughout the utilized spectrum. To illustrate this last sentence, the reader might think of an individual in which one of the channels has a considerably high margin whereas the others present a lower value. Due to the considerably high one-channel margin, this individual might be considered by the algorithm as a candidate solution, when, for practical reasons, this solution is not interesting because some carriers might be at the imminent risk of becoming out of service.

In a similar way to the previous section, two opposing solutions are analyzed in Fig. 6. The solution that prioritizes the bandwidth Fig. 6 is also fully composed by PM-32QAM channels. However, an irregular power spectrum distribution is found. The same happens to Fig. 6.b, but now filled out with PM-4QAM channels. This uneven power spectrum density is a direct cause of the margin distribution inequality problem as discussed in the last paragraph.

The major advantage of deriving a Pareto analysis for the so far cited optimization problems is the generation of multiple close-to-optimal solutions rather than one single exact solution (achieved via strict mathematical programming). As the reader could notice, all solutions on the Pareto's curve (Fig. 4) may represent a specific network requirement that is not only bandwidth or margin-greedy. Table 3 summarizes the values of the objectives for the two individuals (Fig. 6.a,b).

Relation between individual and objective function			
Individual represented by	Sum of SNR Margin (linear)	SNR Margin (dB)	
Fig. 8	18.5	0.14	

**Table 4**

Quantitative comparison between the individuals (Fig. 8) and their respective values of objective functions. BW: bandwidth.

### 3.5. Sum of SNR Margin vs. Minimum SNR Margin

The third and last optimization approach discussed in this paper leads to interesting results in terms of a key requirement in current network scenarios, i.e., provisioning of close-to-zero margin solutions. Therefore, this section will analyze what happens when the minimization of the sum of SNR margins is regarded in a Pareto analysis with the maximization of the lowest SNR margin.

This assumption is clearly conflicting given that when the minimization of the sum of SNR margins is imposed, it consequently lowers the margin of the worst channel, which is the contrary goal of the second objective. Additionally, the minimization of the sum of SNR margins is a subtle way of incorporating the low bandwidth requirement into this analysis (by using high modulation formats it decreases the total margin and reduces bandwidth). Therefore, these solutions are expected to meet more realistic network demands than the one introduced in [6].

In Fig. 7 it can be observed the Pareto's front for the configuration so far discussed. When the solution that prioritizes the minimization of the sum of SNR margins is analyzed (Fig. 8) it is more notorious the diversity of modulation formats that can be utilized. This is due to the fact that the conflicting objective is the maximization of the minimum SNR margin, which strongly imposes the algorithm to also include channels with lower SE (i.e., PM-4QAM and PM-8QAM). Table 4 summarizes the values of the objectives for the individual represented by (Fig. 8).

To check the validity of this optimization approach, a scaling of the network length is proposed and bandwidth reduction is directly contrasted with the results presented in [6].

### 3.6. Scaling point-to-point

In this scaled analysis, each source-destination pair has six channels and the impact of link length is evaluated for the case when a transmission of 200/400 Gbps per channel is performed. Since the focus is to analyze the bandwidth reduction, the solution that prioritizes the minimization of the sum of SNR margins is the one evaluated, given that these two objectives are closely related, as explained before.

A comparison was carried out to contrast the bandwidth usage as the number of spans increases. As Fig. 9 depicts, the algorithm proposed in this work shows a more subtle

bandwidth growth rate. Although for a number of spans lower than 20 (200 Gbps/ch case), and 19 (400 Gbps/ch case) the performance of the algorithm is predominantly worse (generally requiring more bandwidth), this changes when the network size is greater than or equal to 21 (200 Gbps/ch case), and 20 spans (400 Gbps/ch case). The reason for a worse performance is because the NSGA-II forces diverse solutions via the mutation process. That being said, the proposed technique still provides a few high-bandwidth channels for short spans (<19), what could be understood as residual features, although causing higher spectral consumption. Nevertheless, this diversity exploration becomes important at a high number of spans, because it permits that high-order modulations be allocated to provide bandwidth savings when the network size is greater or equal to 21 (200 Gbps/ch case) and 20 spans (400 Gbps/ch case). In proportional terms, the average bandwidth reduction within the better performance interval caused by the utilization of this algorithm is of 60.6% (200 Gbps/ch case) and 61.0% (400 Gbps/ch case).

## 4. Meshed network approach

In this section, the studied technique is adapted to be used in meshed network applications. First, a traditional RSA (routing and spectrum assignment) strategy was upgraded to consider the physical layer. After that, the NSGA-II was implemented to optimize the best set of modulation formats and launch power for all requests in the network, aiming to minimize the number of blocked channels and bandwidth usage. The proposed technique was assessed in ring networks and 15 different meshed topologies leading to significant improvement in bandwidth usage without blocking any additional requests.

Under physical impairment awareness, a key parameter to be satisfied is the minimum required signal-to-noise ratio ( $SNR_{thr}$ ) [5], which has been widely discussed in the previous sections. Signals with SNR above its  $SNR_{thr}$  satisfy the SLA (service level agreement) after Hard-Decision Forward Error Correction (HD-FEC). Therefore, this means that a channel must be blocked if its SNR is below the  $SNR_{thr}$  for a given modulation format.

The traditional RSA paradigm aims at finding the most appropriate routes in terms of minimizing request blocking (percentage of unestablished connections) at the network layer. There may exist more than one shortest-path route (referred to this paper as candidate route –  $R_C$ ) for each source-destination pair (SDP) in the network. In this manuscript, we employed the heuristic Shortest Path with Maximum Spectrum Reuse (SPSR) [19]. Here, the steps to choose a solution for each source and destination pair are described as follows. 1) Assign cost 1 for all links and run Dijkstra [20] algorithm for all SDPs to find the possible routes. 2) In case more than one possible route exists, one is randomly chosen. 3) All SDPs in the network are ordered in a descending order with respect to the amount of links assigned to the SDP. 4) Following that order, the number of

slots requested for each SDP is allocated using the First-Fit (FF) algorithm. It is also important to highlight that all continuity and contiguity constraints are considered in this process.

All RSA algorithms originally assume that the number of required slots is given beforehand for each SDPs. However, in reality, what is given is the bit rate. The modulation format is chosen by the operator and the proposed aim of this work is to guide the choice of parameters, such as modulation format and channel launch power, to further increase the signal SNR and reduce the total bandwidth.

---

#### Algorithm 3 Modulation Format Definition Strategy

---

**Input:** Bit Rate, Launch Power, and SNR Margin of all requests;

**Output:** Modulation format and set of required number of slots ( $T$ ) per request.

```

1:  $Block \leftarrow 0$ 
2:  $T \leftarrow \emptyset$ 
3:  $\Delta SNR \leftarrow$  SNR Margin
4:  $N \leftarrow$  total number of requests
5: for  $i = 1$  to  $N$  do
6:    $Mod \leftarrow$  the highest modulation format available (64 in the case of PM-64QAM)
7:    $ok \leftarrow 0$ 
8:   while  $ok = 0$  do
9:     SNR  $\leftarrow$  Calculate SNR considering only ASE and SCI
10:    if  $SNR - \Delta SNR > SNR_{thr}(Mod)$  then
11:       $M_i \leftarrow Mod$ 
12:       $t_i \leftarrow \frac{BitRate}{2^{B_{Ref} \cdot \log_2 M_i}}$ 
13:       $T \leftarrow T \cup t_i$ 
14:       $ok \leftarrow 1$ 
15:    else
16:      if  $Mod =$  the lowest modulation format available (4 in the case of using PM-QPSK) then
17:         $Block \leftarrow Block + 1$ 
18:         $ok \leftarrow 1$ 
19:      else
20:         $Mod \leftarrow Mod/2$ ; next modulation format available is assigned to be tested
21:      end if
22:    end if
23:  end while
24: end for

```

---

If just ASE and SCI are considered, since they depend on the signal properties and the sequence of links used for transmitting it, their effects on the chosen route can be estimated, the modulation format can be defined, and consequently, the number of slots can be previously computed. However, under the influence of XCI, the relative position of the neighboring connections and their modulation formats directly affect the XCI intensity of the  $i$ -th request that is under investigation. This makes the choice of the modulation format (and consequently the

---

#### Algorithm 4 Final calculation of total blocked channels in the network

---

**Input:** Central frequency of all requests, launch powers, set of routes and bandwidth per request ( $SP$ )s and set of modulation formats ( $M_i$ ) for each  $i$ -th request;

**Output:** Total number of blocked requests in the network;

```

1:  $N \leftarrow$  Total number of requests;
2: for  $i = 1$  to  $N$  do
3:    $SNR_i \leftarrow$  SNR of the  $i$ th request is calculated.
4:   if  $SNR_i < SNR_{thr}(M_i)$  then
5:      $Block \leftarrow Block + 1$ ;
6:     Request  $i$  is deleted of the set  $SP$ ;
7:   end if
8: end for

```

---

number of slots) of the  $i$ -th request dependent on the routing, spectrum positioning and assigned modulation format (RMSA) of other (interfering) connections in the network, which consequently depend on the previous RMSA choices. All this complicates the RMSA problem.

To overcome this issue, we propose an adapted SPSR. In the proposed heuristic, a modulation format is selected such that SNR threshold ( $SNR_{thr}$ ) is not violated by considering ASE and SCI effects on each connection. Additionally, an SNR margin ( $\Delta SNR$ ) to each request is assumed to (indirectly) account for the XCI generated by neighboring channels. A more detailed description is given in the following paragraph.

In Algorithm 3, all requests ( $N$ ) are initialized (line 4) with PM-64QAM as modulation format (line 6). After that, an iterative process to define the assignment of the final modulation format starts (line 8). The connection is sequentially tested if its SNR is higher than  $SNR_{thr} + \Delta SNR$  (line 10). In case it succeeds, the tested candidate modulation format is assigned (line 11) and the algorithm proceeds to check the next request (setting the flag  $ok = 1$  in line 14). When the margin condition is not achieved (line 15), the immediately inferior (i.e., less spectrally efficient) modulation format is assigned (line 19) and re-checked (in line 10). In case the least spectrally efficient modulation format is reached (line 16), blocking occurs.

This interactive process is performed along the RSA process, searching for the most spectral efficient modulation format that fulfills the above conditions to calculate the required number of slots of each connection. With the definition of routes and the required number of slots per request, a second phase starts to establish the requests in the network spectrum and account for the XCI effect. The first-fit spectrum assignment algorithm is used to establish the demands in the network and all central frequencies per request. After that, the real XCI effect on the connections is then quantified by the Algorithm 4. If the  $SNR_{thr}$  of a connection is not satisfied (line 4), it is referenced in this manuscript as a blocked channel and it will not be considered in the calculation of the spectrum

**Algorithm 5** *SPSR with the same Launch Power and SNR margin*

**Input:** All Source-Destination requests, Bit rate, Launch Power, SNR margin;

**Output:** Network Spectrum usage, set of route and bandwidth per requests ( $SP_{best}$ ), number of blocked requests in the network and routes per request;

```

1:  $B_{best} \leftarrow \infty$ ;
2:  $u_{best} \leftarrow \infty$ ;
3:  $SP_{best} \leftarrow \emptyset$ ;
4: for Power = -5 to 5 dBm, with steps of 0.5 dB do
5:   for SNR margin = 0 to 5 dB, with steps of 0.5 dB do
6:      $SP \leftarrow \emptyset$ ;
7:      $M_i \leftarrow$  modulation format of request  $i$ 
8:     Dijkstra's algorithm is used to define the shortest
       route ( $P$ ) for each source-destination request in the
       network;
9:     Algorithm 3 is used to determine, for each request,
       the modulation format with the highest SE that
       satisfies QoT criteria. The set  $T$  that records all
       demanded number of slots ( $t_i$ ) for each  $i$  request is
       created.
10:     $SP \leftarrow \langle P, T \rangle$  for all requests not blocked;
11:    The FF algorithm is used to allocate the requests in
       the network;
12:    Algorithm 4 measures the number of blocked
       channels on the network ( $Block$ ) by including XCI,
       and defines the final set  $SP$ .
13:    Network Spectrum usage ( $u$ ) is defined for the final
       set  $SP$  as the number of slots used in the spectrum
       on the network.
14:    if ( $Block \leq B_{best}$ ) and ( $u \leq u_{best}$ ) then
15:       $B_{best} \leftarrow Block$ ;
16:       $u_{best} \leftarrow u$ ;
17:       $SP_{best} \leftarrow SP$ ;
18:    end if
19:  end for
20: end for
21: The  $SP_{best}$  is the final solution used;
```

usage (line 6).

The next step in our proposed method is to better select the parameters (predicted SNR margin and power level) of the requests, for that an optimization scheme must be devised. Since a grid-search approach is costly in terms of computational effort and time due to the high number of possibilities to be tested, this paper utilizes the NSGA-II approach, already introduced in the previous sections, to set the launch power and SNR margin ( $\Delta SNR$ ) for each SDP in the network, aiming at reducing the total number of blocked channels and total bandwidth usage.

#### 4.1. Evolutionary RMLSA approach (E-RMLSA)

The method introduced in this section is a strategy to optimize the choice of connection SNR margins and power level, which impacts the provisioning performance. We

have named this novel approach as Evolutionary RMLSA (E-RMLSA). In order to highlight the importance of the power allocation and SNR margin distribution in network planning, this work uses as baseline the case where both referred parameters (power level and SNR margin) are constant. This baseline scenario is further described by the Algorithm 5.

**Algorithm 6** *Objective Function for the individual (I, J) - E-RMLSA*

**Input:** Population  $Q$ , Network Topology, Bit rate requested

**Output:** Network Spectrum usage, set of routes and bandwidth per requests ( $SP_{best}$ ), number of blocked requests in the network and routes / modulation format per request;

```

1: for  $a = 1$  to  $4N$  do
2:    $I_a \leftarrow$  Set of Launch Powers of the individual  $a$ 
3:    $J_a \leftarrow$  Set of SNR margin of the individual  $a$ 
4:    $Block \leftarrow 0$ ;
5:    $u \leftarrow 0$ ;
6:    $k \leftarrow$  number of source-destination requests in the
       topology;
7:   Dijkstra's algorithm is used to define the shortest
       route ( $P$ ) for each source-destination request in the
       network;
8:   for  $Request = 1$  to  $k$  do
9:      $Pot(Request) \leftarrow I_a(Request)$ ;
10:     $SNR.Margin(Request) \leftarrow J_a(Request)$ ;
11:  end for
12:  Algorithm 3 is used to determine, for each request,
       the modulation format with the highest SE that
       satisfies QoT criteria. The set  $T$  that records all
       demanded number of slots ( $t_i$ ) for each  $i$  request is
       created.
13:   $SP \leftarrow \langle P, T \rangle$  for all requests not blocked;
14:  The FF algorithm is used to allocate the requests in
       the network;
15:  Algorithm 4 measures the number of blocked
       channels in the network ( $Block$ ) by including XCI,
       and defines the final set  $SP$ .
16:  Network Spectrum usage ( $u$ ) is defined for the final
       set  $SP$  as the number of slots used in the spectrum
       on the network.
17:   $B_a \leftarrow Block$ ;
18:   $u_a \leftarrow u$ ;
19: end for
```

In Algorithm 5, all connections are initialized with the same power level (line 4), which can be a discrete value in the set  $\{-5, \dots, 5\}$  dBm with a fixed step of 0.5 dB. With respect to the SNR margin, the same strategy is also applied, where each connection can assume a discrete value in the set  $\{0, \dots, 5\}$  dB, with steps of 0.5 dB. After Dijkstra's algorithm is applied to compute the shortest path, Algorithm 3 is called to determine the modulation formats to be used (Algorithm 5 line 9). In sequence, the FF algorithm emulates the allocation of connections (line 11)

and finally the number of blocked channels is assessed via Algorithm 4 (line 12). The final blocking (*blocking*) and spectrum utilization ( $u$ ) are saved only if these are the best values for all combinations tested in the grid-search so far (line 14). This exhaustive method is used in the optimization process.

In Sec. 2, NSGA-II was introduced as a method to optimize some of the parameters (modulation format, launch power) in the physical layer. Now it is brought to a network layer perspective. The same stages: initialization, mutation, and crossover have been reprocessed. The adaption made for the network is that now each individual on the NSGA-II is a set of all SDP of the network with different features per SDP defined as launch power and SNR margin. This means that each NSGA-II individual is one feasible solution for the full planning of our network, i.e., it takes into account all network requests. Since the planning is based on a static traffic (all requests are known *a priori*) each possible request (source-destination pair) is treated as a gene with two features, namely, (1) launch power and (2) SNR margin.

Therefore, in the objective function, each individual is evaluated based on the total spectrum occupied by all network requests and the number of blocked channels (for a full simulation run). The E-RMLSA objective function is introduced in Algorithm 6. Finally, the evolutionary algorithm comes to play the role of finding the best distribution of those features to reduce both the number of channels blocked and the bandwidth usage in the network. This means that in this multi-optimization scenario, blocking and spectral usage are jointly minimized using the Pareto concept described in the Sec. 2.

Moreover, it is important to highlight that, for all simulations exposed in this section, the network spectrum on fiber links was assumed with a spectrum resolution of 3.125 GHz, for comparative reasons with the work in [7]. Likewise, we have assumed that there is a traffic demand between each source–destination pair, for which the data rate is 100 Gbps. In addition, in our simulator, each link consists of two fiber spans and just one traffic demand as in [7]. All network system parameters are the same of Sec. 3. In the next subsection, the results for ring and meshed networks are presented.

#### 4.1.1. Ring Networks

In [7], it was presented a joint resource allocation in flexible-grid networks based on a nonlinear physical layer impairment model. Nevertheless, the method is limited to investigations in ring topology. In this work, the proposed approach is also contrasted with the technique introduced in [7] using the same topology. In Fig. 10, it can be seen that the proposed algorithm can provide further improvements by not imposing guardband adaptation (which consumes more spectral resources), unlike [7]. Still, the algorithm is capable of optimizing the margins (which indirectly decides the choice of the modulation format) and power levels to mitigate the nonlinear impairments. The

**Table 5**  
**Real-world reference networks [21, 22]**

Network ID	Name	$N$	$L$	$\langle \delta \rangle$	Channels
1	BREN [21, 22]	10	11	2.20	90
2	LEARN [21, 23]	10	11	2.20	90
3	ABILENE [24]	11	14	2.55	110
4	COMPUSERVE [25]	11	14	2.55	110
5	VBNS [21, 26]	12	17	2.83	132
6	CESNET [21, 22]	12	19	3.17	132
7	BRAZILIAN [24]	12	20	3.33	132
8	ITALY [21, 27]	14	29	4.14	182
9	PACIFIC BELL [28]	17	23	2.71	272
10	SPAIN [21, 22]	17	28	3.29	272
11	CANARIE [21, 22]	19	26	2.74	342
12	EON [24]	19	38	4.00	342
13	SWEDEN [21, 22]	20	24	2.40	380
14	ARPANET [21, 29]	20	32	3.20	380
15	PIONIER [21, 22]	21	50	4.76	420

relative bandwidth reductions are on average (from 0 to 8 nodes) around 14%.

#### 4.1.2. Mesh Networks

Now the Algorithm 5 is applied to meshed networks. For the sake of generality, the tests were carried out in 15 different network topologies. Table 5 reports the important information (number of nodes, number of links, nodal degree, number of connections, and references) for all networks considered in this paper. The result is summarized in Fig. 11 and it shows the achieved spectrum saving in GHz (red bars) with respect to the grid-search approach (Algorithm 5). We have achieved gains in the range of 100 GHz to 1100 GHz. As can be seen in Fig. 11, the gain does not depend only on the size of the network but also on how the network is interconnected. To evaluate the interconnectivity of all networks, we have calculated the nodal degree ( $\langle \delta \rangle$ ) and their values are likewise represented in Table 5. Two major conclusions can be drawn from the outcomes shown in Fig. 11.

First, for networks with the same number of nodes, the performance increases with the nodal degree. This effect is particularly clear in EON and Canarie networks, where both of them have 19 nodes, but since the EON has a higher nodal degree, the gain compared with the Canarie was approximately twice higher. The reason for this is that higher nodal degree means more connected links per node, which will provide more variety of possibilities for the NSGA-II to identify better launch power and SNR margin for each SDP.

Second, the performance grows with the number of nodes and it is directly related to the number of channels in the network up to a certain point when we observe a decrease of the gain, as presented by the green dashed line in Fig. 11. The reason for it lies in our approach that guesses the probable contribution of XCI to the SNR margin. With the increase of the number of channels, XCI becomes stronger with impact on the effectiveness of the

strategy that calculates ASE and SCI but only guesses XCI with the evolutionary method.

## 5. Conclusion

In this paper, we presented a novel resource allocation technique as a means to optimize the usage of spectrum resources and power allocation in flexible-grid link-level and meshed networks under nonlinear physical impairment regime. The similarity between optical spectrum and genetic features helps the implementation of an evolutionary-based optimization technique that permits a trade-off analysis in multi-objective scenarios. Due to the demanding network requirements to reduce SNR-margin, a reformulation of a key optimization premise, i.e., minimization of the sum of SNR margins, leads to solutions in which the bandwidth can be saved, on average, by 61%, at the cost of excluding the guardband between channels. Additionally, when the algorithm is adapted to ring networks, it overperforms the baseline by reducing the spectrum usage in 14%. At last, the algorithm is shown to be fit for the planning of networks with static traffic when various meshed topologies are tested demonstrating significant gain in spectral utilization.

Finally, the authors believe that future follow-up approaches for the implementation presented in this manuscript include the incorporation into the NSGA-II of "*a priori*" knowledge to speed up evolutionary learning. To illustrate, we showed in this research that the majority of links with fewer spans can support lower SNR margins (e.g., using modulation formats with lower SE) than those links with a high number of spans. This "*a priori*" conditioning could be embedded in the initialization process, where each individual receives its initial features according to the link characteristics.

## 6. Acknowledgments

This work has received partial funding from the EU Horizon 2020 program under the Marie Skłodowska-Curie grant agreement No. 813144 (REAL-NET) and the Brazilian National Council for Scientific and Technological Development (CNPq), as well as the institutional support from UFPE and UFBA.

## References

- [1] J. Zhao, H. Wymeersch, E. Agrell, Nonlinear impairment aware resource allocation in elastic optical networks, in: Optical Fiber Communication Conference, Optical Society of America, 2015, pp. M2I-1.
- [2] E. Palkopoulou, G. Bosco, A. Carena, D. Klonidis, P. Poggiolini, I. Tomkos, Nyquist-wdm-based flexible optical networks: Exploring physical layer design parameters, Journal of Lightwave Technology 31 (14) (2013) 2332–2339.
- [3] P. Poggiolini, G. Bosco, A. Carena, V. Curri, Y. Jiang, F. Forghieri, The gn-model of fiber non-linear propagation and its applications, Journal of lightwave technology 32 (4) (2013) 694–721.
- [4] K. V. Peddanarappagari, M. Brandt-Pearce, Volterra series transfer function of single-mode fibers, Journal of lightwave technology 15 (12) (1997) 2232–2241.
- [5] D. J. Ives, P. Bayvel, S. J. Savory, Adapting transmitter power and modulation format to improve optical network performance utilizing the gaussian noise model of nonlinear impairments, Journal of Lightwave Technology 32 (21) (2014) 3485–3494.
- [6] L. Yan, E. Agrell, H. Wymeersch, M. Brandt-Pearce, Resource allocation for flexible-grid optical networks with nonlinear channel model, Journal of Optical Communications and Networking 7 (11) (2015) B101–B108.
- [7] L. Yan, E. Agrell, H. Wymeersch, P. Johannisson, R. Di Taranto, M. Brandt-Pearce, Link-level resource allocation for flexible-grid nonlinear fiber-optic communication systems, IEEE Photonics Technology Letters 27 (12) (2015) 1250–1253.
- [8] L. Pavel, Osnr optimization in optical networks: Modeling and distributed algorithms via a central cost approach, IEEE Journal on Selected Areas in Communications 24 (4) (2006) 54–65.
- [9] M. Schaedler, M. Kuschnerov, S. Pachnicke, C. Bluemmm, F. Pittala, X. Changsong, Subcarrier power loading for coherent optical ofdm optimized by machine learning, in: Optical Fiber Communication Conference, Optical Society of America, 2019, pp. M2H-3.
- [10] M. R. Sena, J. R. Mendes, R. C. Almeida, P. J. Souza, An evolutionary method to optimize osnr margin in elastic optical channels subject to nonlinear physical impairments, in: 2018 SBFoton International Optics and Photonics Conference (SBFoton IOPC), IEEE, 2018, pp. 1–5.
- [11] R. Morais, C. Pavan, A. Pinto, C. Requejo, Genetic algorithm for the topological design of survivable optical transport networks, IEEE/OSA Journal of Optical Communications and Networking 3 (1) (2011) 17–26. doi:10.1364/JOCN.3.000017.
- [12] M. Mitchell, An introduction to genetic algorithms, MIT press, 1998.
- [13] P. Bonami, L. T. Biegler, A. R. Conn, G. Cornuéjols, I. E. Grossmann, C. D. Laird, J. Lee, A. Lodi, F. Margot, N. Sawaya, et al., An algorithmic framework for convex mixed integer nonlinear programs, Discrete Optimization 5 (2) (2008) 186–204.
- [14] A. Xavier, R. Silva, D. Chaves, C. Bastos-Filho, R. Almeida, J. Martins-Filho, The nrpsr-elastic routing algorithm for flexible grid optical networks, in: 2013 SBMO/IEEE MTT-S International Microwave & Optoelectronics Conference (IMOC), IEEE, 2013, pp. 1–5.
- [15] L. Yan, E. Agrell, M. N. Dharmaweera, H. Wymeersch, Joint assignment of power, routing, and spectrum in static flexible-grid networks, Journal of Lightwave Technology 35 (10) (2017) 1766–1774.
- [16] W. Kim, Adaptive weighted sum method for multiobjective optimization: a new method for Pareto front generation, Vol. 2, 2005.
- [17] E. Zitzler, Evolutionary algorithms for multiobjective optimization: Methods and applications, Vol. 63, Citeseer, 1999.
- [18] T. T. Joy, S. Rana, S. Gupta, S. Venkatesh, Hyperparameter tuning for big data using bayesian optimisation, in: 2016 23rd International Conference on Pattern Recognition (ICPR), 2016, pp. 2574–2579. doi:10.1109/ICPR.2016.7900023.
- [19] Y. Wang, X. Cao, Q. Hu, Y. Pan, Towards elastic and fine-granular bandwidth allocation in spectrum-sliced optical networks, J. Opt. Commun. Netw. 4 (11) (2012) 906–917. doi:10.1364/JOCN.4.000906. URL <http://jocn.osa.org/abstract.cfm?URI=jocn-4-11-906>
- [20] E. W. Dijkstra, et al., A note on two problems in connexion with graphs, Numerische mathematik 1 (1) (1959) 269–271.
- [21] Real-world optical transport network topologies, <http://www.av.it.pt/anp/on/refnet2.html>.
- [22] C. Pavan, R. M. Morais, J. R. Ferreira da Rocha, A. N. Pinto, Generating realistic optical transport network topologies, IEEE/OSA Journal of Optical Communications and Networking 2 (1) (2010) 80–90.
- [23] S. K. Routray, R. M. Morais, J. R. F. da Rocha, A. N. Pinto, Statistical model for link lengths in optical transport networks, IEEE/OSA Journal of Optical Communications and Networking 5 (7) (2013) 762–773.
- [24] K. D. R. Assis, A. F. dos Santos, R. C. A. Jr., Optimization in spectrum-sliced optical networks, in: Optical Metro Networks

and Short-Haul Systems VI, International Society for Optics and Photonics, SPIE, 2014, pp. 102 – 109. doi:10.1117/12.2040472.  
URL <https://doi.org/10.1117/12.2040472>

- [25] D. T. Hai, An optimal design framework for 1 + 1 routing and network coding assignment problem in wdm optical networks, *IEEE Access* 5 (2017) 22291–22298.
- [26] R. Bartos, M. Raman, A heuristic approach to service restoration in mpls networks, in: *ICC 2001. IEEE International Conference on Communications. Conference Record (Cat. No.01CH37240)*, Vol. 1, 2001, pp. 117–121 vol.1.
- [27] D. Colle, S. De Maesschalck, C. Develder, P. Van Heuven, A. Groebbens, J. Cheyns, I. Lievens, M. Pickavet, P. Lagasse, P. Demeester, Data-centric optical networks and their survivability, *IEEE Journal on Selected Areas in Communications* 20 (1) (2002) 6–20.
- [28] M. M. Alves, R. C. Almeida Jr, A. F. dos Santos, H. Pereira, K. D. Assis, Impairment-aware fixed-alternate bsr routing heuristics applied to elastic optical networks, *JOURNAL OF SUPERCOMPUTING*.
- [29] Tong Ye, Qingji Zeng, Yikai Su, Lufeng Leng, Wei Wei, Zhizhong Zhang, Wei Guo, Yaohui Jin, On-line integrated routing in dynamic multifiber ip/wdm networks, *IEEE Journal on Selected Areas in Communications* 22 (9) (2004) 1681–1691.

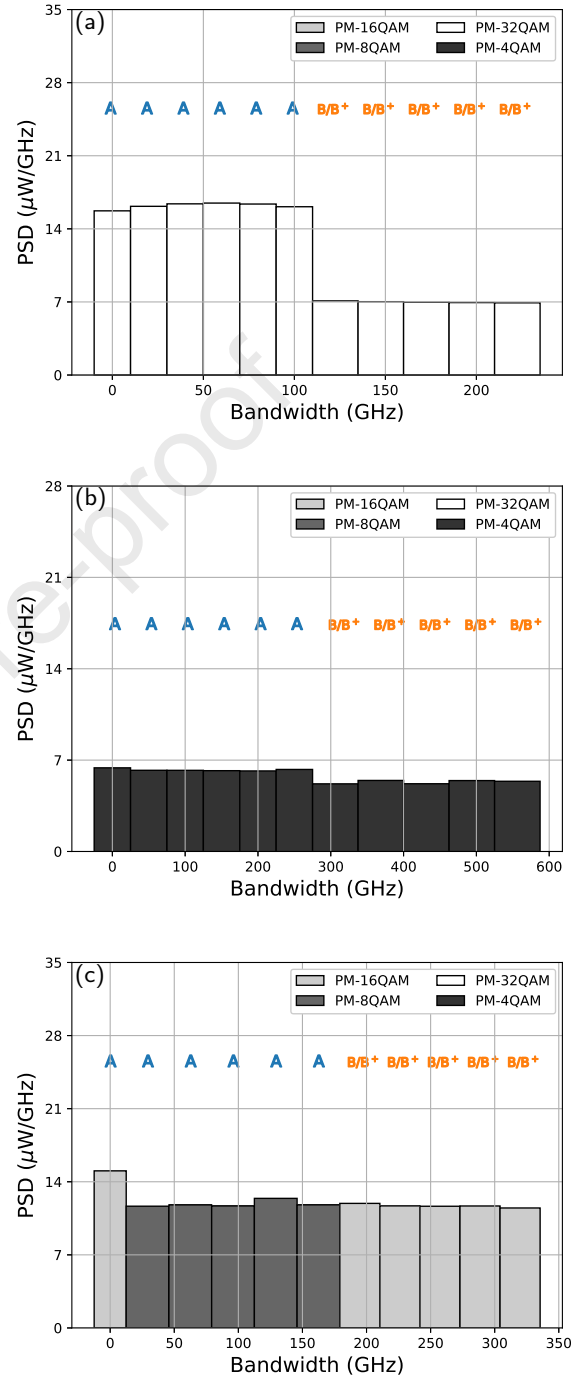


**Figure 5:** Samples of solutions from the Total bandwidth vs. Minimum SNR Margin Pareto analysis. (a) Individual that prioritizes bandwidth reduction over maximizing minimum SNR; (b) Individual that prioritizes maximizing minimum SNR over bandwidth reduction; (c) Individuals with intermediate profile. PSD: Power spectrum density.

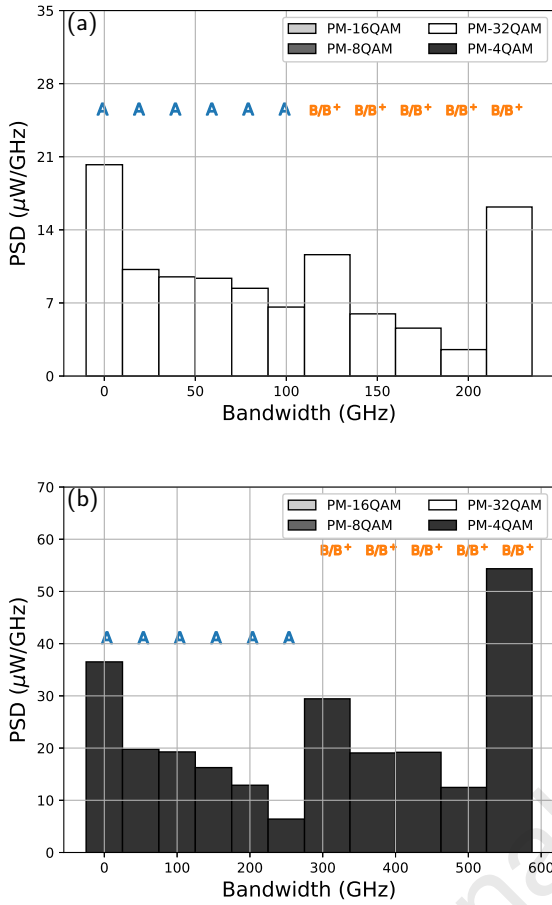


**Figure 6:** Samples of solutions from the Total bandwidth vs. Sum of SNR Margin multi-optimization. (a) Individual that prioritizes bandwidth reduction over maximizing sum of SNR margin; (b) Individual that prioritizes maximizing the sum of SNR margins over bandwidth reduction. PSD: Power spectrum density.

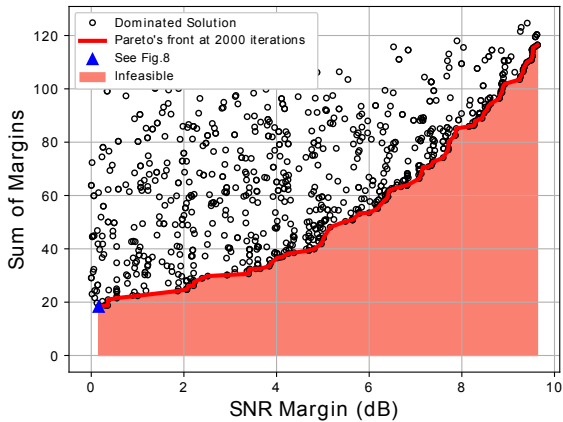


**Figure 7:** Pareto's front for the multi-objective optimization. Sum of SNR Margin vs. Minimum SNR Margin.

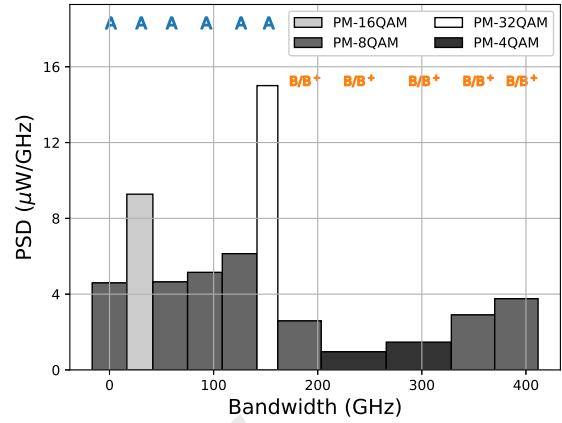


**Figure 8:** Individual that prioritizes minimizing sum of SNR margins over maximization of lowest SNR margin. PSD: Power spectrum density.

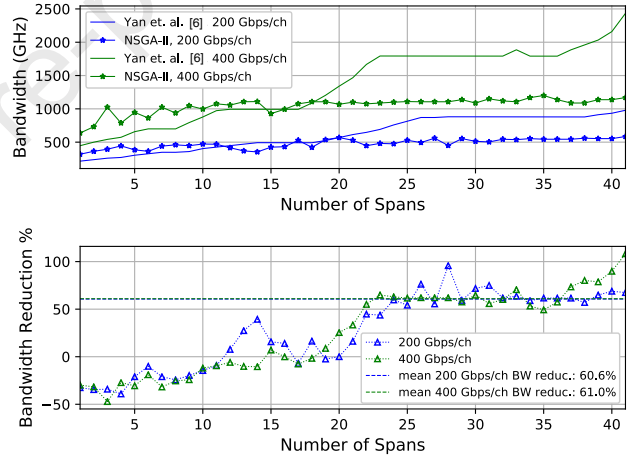


**Figure 9:** Bandwidth consumption as a function of the transmission distance.

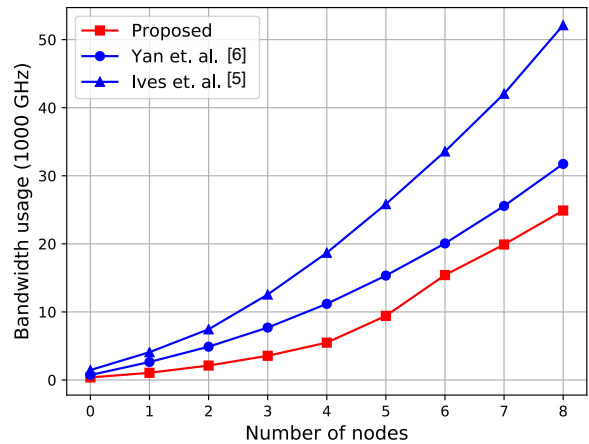


**Figure 10:** Bandwidth usage with respect to number of nodes.

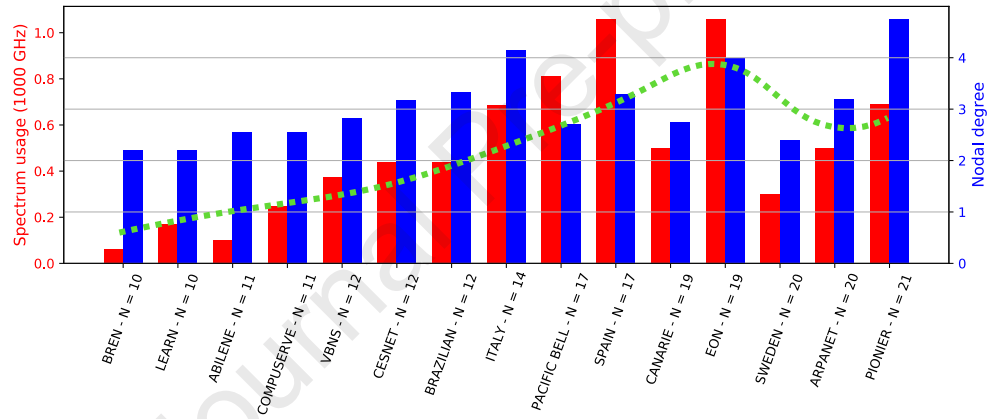


**Figure 11:** Spectral usage reduction and nodal degree as function of the meshed network topologies. The dashed green curve visualizes the average response of the spectrum usage.

**Declaration of interests**

The authors declare that they have no known competing financial interests or personal relationships that could have appeared to influence the work reported in this paper.

The authors declare the following financial interests/personal relationships which may be considered as potential competing interests:

Journal Pre-proof